

Nes2Net: A Lightweight Nested Architecture for Foundation Model Driven Speech Anti-spoofing

Tianchi Liu, *Student Member*, Duc-Tuan Truong, *Student Member*, Rohan Kumar Das, *Senior Member*, Kong Aik Lee, *Senior Member*, Haizhou Li, *Fellow*

Abstract—Speech foundation models have significantly advanced various speech-related tasks by providing exceptional representation capabilities. However, their high-dimensional output features often create a mismatch with downstream task models, which typically require lower-dimensional inputs. A common solution is to apply a dimensionality reduction (DR) layer, but this approach increases parameter overhead, computational costs, and risks losing valuable information. To address these issues, we propose Nested Res2Net (Nes2Net), a lightweight back-end architecture designed to directly process high-dimensional features without DR layers. The nested structure enhances multi-scale feature extraction, improves feature interaction, and preserves high-dimensional information. We first validate Nes2Net on CtrSVDD, a singing voice deepfake detection dataset, and report a 22% performance improvement and an 87% back-end computational cost reduction over the state-of-the-art baseline. Additionally, extensive testing across four diverse datasets—ASVspoof 2021, ASVspoof 5, PartialSpoof, and In-the-Wild—covering fully spoofed speech, adversarial attacks, partial spoofing, and real-world scenarios, consistently highlights Nes2Net’s superior robustness and generalization capabilities. The code package and pre-trained models are available at <https://github.com/Liu-Tianchi/Nes2Net>.

Index Terms—DeepFake detection, speech anti-spoofing, Res2Net, Nes2Net, SSL, speech foundation model

I. INTRODUCTION

SPEECH foundation models, such as wav2vec 2.0 [1], HuBERT [2], and WavLM [3], have revolutionized speech processing by leveraging large-scale pretraining to capture complex acoustic and linguistic patterns [4]. This has driven notable advances in automatic speech recognition (ASR) [5], speaker verification (SV) [6], and other speech applications.

Beyond traditional tasks, speech foundation models also show great promise in addressing critical security concerns, particularly speech anti-spoofing (also referred to as deepfake detection) [7]. With the growing sophistication of spoofing techniques, such as voice conversion, ensuring the reliability and security of speech-driven systems has become a pressing

concern [8]–[12]. Leveraging the rich representations of these foundation models could significantly improve the robustness and generalization of anti-spoofing systems [13]–[15].

While the speech foundation models offer exceptional representations, their high-dimensional feature outputs present significant challenges for downstream tasks. Downstream models used in tasks like speech anti-spoofing typically require lower-dimensional features [15]–[17]. To address this mismatch, a common approach is to introduce a dimensionality reduction (DR) layer, usually implemented as a fully connected (FC) layer for transforming high-dimensional features into lower-dimensional features. However, this conventional strategy presents notable drawbacks. Since downstream classifiers are usually compact, the DR layer alone often consumes a substantial portion of the parameters and computational resources within the entire back-end model. Moreover, directly projecting high-dimensional features in a one-shot manner through an FC layer leads to the loss of important information, reducing the effectiveness of speech foundation models. These issues highlight the need for a more efficient and effective solution to bridge the dimensionality gap and fully utilize speech foundation models in downstream tasks.

To address these challenges, we propose Nested Res2Net (Nes2Net) to process high-dimensional features from speech foundation models, eliminating the need for a DR layer while preserving the richness of the original representations. By addressing key limitations of DR layers, such as excessive computational cost and information loss, Nes2Net offers a more efficient and effective solution. This design makes it particularly suitable for tasks requiring a balance of high performance and efficiency, such as speech anti-spoofing. The key contributions of this work can be summarized as follows:

- **Novel Architecture:** We introduce Nes2Net, a new approach that effectively addresses the limitations of DR layers. Nes2Net retains the expressive power of high-dimensional features while reducing model complexity.
- **Enhanced Performance, Efficiency, and Generalization:** Our method demonstrates significant improvements in efficiency, achieving performance improvements of 22% while reducing computational costs by 87% compared to the SOTA baseline on the CtrSVDD dataset. Further experiments conducted on four additional datasets across various scenarios demonstrate strong generalization capability and consistently superior performance.
- **Reproducibility:** To facilitate further research and application, we make our scripts and pre-trained models publicly available.

Tianchi Liu and Haizhou Li are with the Department of Electrical and Computer Engineering, National University of Singapore, Singapore. Tianchi Liu is also with LIGHTSPEED, Singapore. (email: tianchi_liu@u.nus.edu);

Duc-Tuan Truong is with the Nanyang Technological University, Singapore. (email: truongdu001@e.ntu.edu.sg);

Rohan Kumar Das is with the Fortemedia Singapore, Singapore. (email: ecerohan@gmail.com);

Kong Aik Lee is with the Department of Electrical and Electronic Engineering, The Hong Kong Polytechnic University, Hong Kong. (e-mail: kong-aik.lee@polyu.edu.hk);

Haizhou Li is also with the School of Data Science, Shenzhen Research Institute of Big Data, The Chinese University of Hong Kong, Shenzhen, China. (email: haizhouli@cuhk.edu.cn);

II. RELATED WORK

A. Res2Net

Res2Net [18] is a well-known architecture designed to extract multi-scale features. Unlike ResNet [19], Res2Net uses hierarchical residual connections within a single block, allowing it to capture patterns across varying receptive fields simultaneously [18]. This design offers proven advantages in speech-related tasks, such as SV [20]–[22] and anti-spoofing [23]–[25], where capturing subtle variations and complex acoustic patterns is important. As shown in Fig. 1, Res2Net (highlighted using a light red block) can also serve as a classifier within a speech foundation model-based anti-spoofing system. Its ability to extract multi-scale features has led to superior performance to conventional models, that motivates the design of Nested Res2Net in this work.

B. Traditional Speech Anti-Spoofing Models

Traditional speech anti-spoofing models have evolved to effectively detect speech deepfakes [26], [27]. For instance, the Channel-wise Gated Res2Net (CG-Res2Net) [23] introduces a gating mechanism within the Res2Net architecture, enabling dynamic selection of channel-wise features to enhance generalization to unseen attacks. A widely recognized model among traditional approaches is AASIST [26], which employs spectro-temporal graph attention layers to capture both temporal and spectral artifacts, thereby achieving efficient and accurate detection. Given AASIST’s SOTA performance and its wide adoption in recent anti-spoofing challenges [16], [28], we consider it as our main baseline for evaluation.

Although traditional anti-spoofing models are characterized by their compact size and rapid inference capabilities, they typically rely on hand-crafted acoustic features, which limit their adaptability to diverse spoofing methods. With the rise of deepfakes and adversarial attacks, stronger and more flexible representations are needed.

C. Speech Foundation Models

Speech foundation models, often referred to as Self-Supervised Learning (SSL) models due to their typical pre-training on large amounts of unlabeled speech data using self-supervised learning techniques. Examples include wav2vec 2.0 [1], HuBERT [2], and WavLM [3]. Unlike traditional acoustic feature-based approaches, which rely on hand-crafted features and are often task-specific, SSL models learn rich and generalized speech representations that can be effectively adapted to various downstream applications. This allows them to achieve superior performance in speech-related tasks, including speech anti-spoofing.

D. Speech Foundation Model-based Anti-spoofing

As discussed in the previous subsection, speech foundation models can capture more informative representations than traditional handcrafted or raw acoustic features [3]. This makes them highly effective for speech anti-spoofing, as they generalize well across datasets and are more robust to unseen attacks [15]. As a result, many recent anti-spoofing systems

increasingly adopt these models as front-ends, feeding their features to back-end classifiers and consistently outperforming traditional models [16], [29], [30].

To connect these powerful front-end models to downstream classifiers, a feature aggregation layer is introduced, as shown in Fig. 1. This layer combines features from different SSL layers using methods such as a simple *weighted sum* or attention-based methods like Squeeze-and-Excitation Aggregation (SEA) [16] and Attentive Merging (AttM) [31].

Following the aggregation layer, the resulting features are passed to the back-end classifier, as shown in the green box of Fig. 1. Existing methods typically use a DR layer, which reduces the high-dimensional feature of channel N (commonly $N = 1024$ [1], [3], [32]) to a lower dimension D (e.g., $D = 128$ [15], [16] or $D = 144$ [17], [33]) to match the classifier model’s input requirements. The classifier model then extracts features from the DR layer outputs and produces the final score. As illustrated in the red box of Fig. 1, commonly used classifier structures include traditional models such as ResNet [19], Res2Net [18], ECAPA-TDNN [34], and AASIST [26].

The strong performance of these systems stems from their ability to capture rich speech representations, enabling more accurate distinction between real and spoofed speech. As a result, these systems have achieved SOTA results [33], [35], [36], especially in recent challenges like ASVspoof 5 [28], [37], CtrSVDD [16], [38], [39], and ADD [40]. However, the use of a DR layer introduces challenges that limit the back-end’s ability to fully leverage the rich representations from speech foundation models. In this work, we aim to better unlock the potential of foundation models for speech anti-spoofing. These issues will be discussed in the next subsection.

E. Limitation of Dimensionality Reduction Layer

Existing speech foundation model-based anti-spoofing systems excel in extracting rich, high-dimensional feature representations, which capture intricate patterns in speech. However, this high dimensionality poses a significant challenge for downstream tasks. Models in these tasks typically require lower-dimensional features [23], [26], [27], creating a mismatch between the output features of the foundation models and the requirements of downstream processing.

A commonly used approach for dimensionality reduction is to employ a DR layer. However, this approach has several issues, including parameter overhead and potential information loss. As shown in Table I, our analysis of back-end models further emphasizes the inefficiency of this approach. We consider commonly used feature dimensions of $N = 1024$ from large models [1], [3], and a reduced dimension of $D = 128$, widely adopted in SOTA back-end models [15], [16], [31].

Across various back-end models, the DR layer, despite being just a single layer, consistently accounts for a substantial share of parameters and computational cost, underscoring its resource-intensive nature. For instance, the DR layer accounts for 21% to 29% of the parameters across ResNet, Res2Net, ECAPA, and AASIST. In terms of computational cost, the DR layer generally contributes at least one-third of the total MACs.

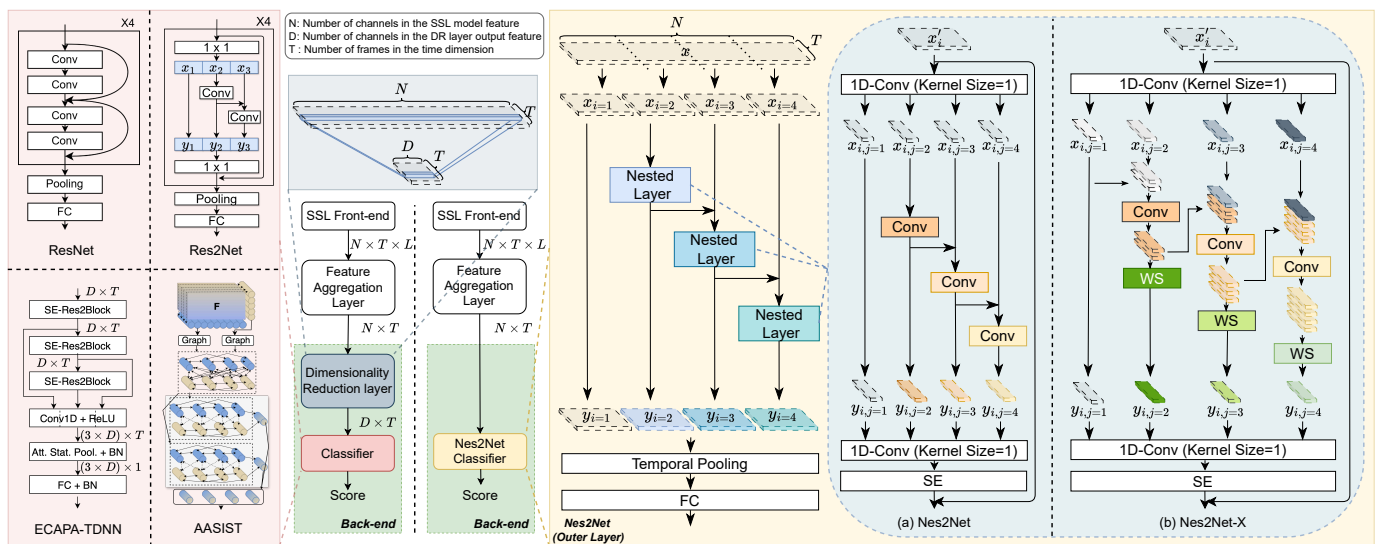


Fig. 1. The block diagram of the speech foundation model-based speech anti-spoofing system, showcasing both the traditional back-end models and the proposed Nes2Net back-end. The traditional back-end models include a DR layer and a classifier, such as ResNet [19], Res2Net [18], ECAPA-TDNN [34], and AASIST [26]. In contrast, the proposed Nes2Net back-end model features a DR layer-free design. Additionally, an enhanced version of its nested layer, named Nes2Net-X, is introduced to further improve performance. Abbreviations used in the figure include: ‘FC’ (fully connected layer), ‘Conv’ (convolutional layer), ‘WS’ (weighted sum), ‘SE’ (squeeze-and-excitation module) [41], and ‘Att. Stat. Pool.’ (attentive statistics pooling) [42].

TABLE I

CONTRIBUTION OF THE DR LAYER ON THE NUMBER OF PARAMETERS AND COMPUTATIONAL COST IN BACK-END MODELS. MMACS STANDS FOR MILLION MULTIPLY-ACCUMULATE OPERATIONS.

| Back-end Model | Parameters | | | MMacs | | |
|----------------|------------|-------|-----|-------|--------|-----|
| | DR | Total | % | DR | Total | % |
| ResNet [19] | 131k | 611k | 21% | 26.24 | 70.62 | 37% |
| Res2Net [18] | 131k | 452k | 29% | 26.24 | 64.93 | 40% |
| ECAPA [34] | 131k | 497k | 26% | 26.24 | 80.21 | 33% |
| AASIST [26] | 131k | 447k | 29% | 26.24 | 707.65 | 4% |

AASIST is the only exception, where the DR layer accounts for just 4% of the MACs, primarily because the overall MACs of AASIST are significantly larger—an order of magnitude higher than those of other models.

This table highlights that a single DR layer significantly inflates the back-end model’s size and resource demands. Furthermore, its direct projection design discards important high-dimensional features, limiting the overall potential of speech foundation models.

III. METHODOLOGY

A. Proposed Nested Res2Net (Nes2Net)

The design of Nes2Net is driven by two primary objectives: 1) effectively and efficiently utilizing the high-dimensional features from speech foundation models, and 2) enhancing multi-scale feature extraction to achieve robust generalization in speech anti-spoofing tasks. These objectives are realized through a novel nested architecture that simultaneously improves the efficiency, flexibility, and robustness of the model.

Efficiency and Retention of Rich Feature Information: The analysis in Section II-E reveals the limitations of employing the DR layer, highlighting its significant computational overhead and potential information loss. These drawbacks motivate the need for a more efficient solution—one that

bridges the dimensionality gap without sacrificing the richness of high-dimensional representations from speech foundation models. To this end, Nes2Net entirely removes the DR layer, directly processing high-dimensional features to retain their intrinsic richness and minimize unnecessary computational costs. By bypassing the DR layer, Nes2Net prevents the information bottleneck typically caused by early dimensionality reduction. This ensures the preservation of detailed representations essential for accurately distinguishing genuine speech from spoofed audio. Furthermore, the nested structure optimizes computational efficiency by systematically refining and managing feature representations across multiple groups, ensuring maximum utilization of high-dimensional features with minimal computational overhead.

Enhanced Multi-Scale Feature Interaction and Expressiveness: While the Res2Net architecture effectively extracts multi-scale features through hierarchical splits, it exhibits significant limitations when processing high-dimensional features directly, especially with large split scales s . Specifically, Res2Net suffers from feature dilution [18], redundant transformations [43], and restricted interactions among channels. Excessive splitting fragments the features, weakening their expressiveness, and repetitive transformations increase computational redundancy, potentially causing overfitting. Moreover, closely related information can be distributed across distant subsets, limiting effective cross-channel interactions.

To overcome these limitations, as illustrated in Fig. 1, we propose a novel **Nested Res2Net (Nes2Net)** architecture that introduces a hierarchical nesting structure. This added degree of flexibility significantly enhances the model’s representational power. Each nested layer progressively refines features by building upon outputs from preceding layers and also incorporates efficient local cross-channel attention mechanisms [44], [45], strengthening interactions across channels. This holistic feature extraction approach enables Nes2Net to

comprehensively capture intricate speech patterns. Moreover, the cumulative refinement effectively mitigates the issue of feature dilution, preserving rich and expressive multi-scale information. Benefiting from the structural advantages of the nesting strategy, the need for excessive fine-grained splits is reduced, effectively mitigating redundant transformations. This approach also minimizes unnecessary computations, resulting in a compact yet highly expressive model.

Critically, overfitting is a well-known challenge in speech anti-spoofing tasks, often leading to degraded performance in cross-domain scenarios. Previous studies [23], [26], particularly with compact models like AASIST and Res2Net (both with fewer than 500k parameters), have shown that smaller models can help reduce overfitting. Our experiments with these models confirm that simply increasing their size does not always lead to better performance and can, in fact, make overfitting worse. As a result, improving feature quality through smarter model structure design becomes more important than just scaling up the model. The nested architecture of Nes2Net provides clear benefits—it maintains computational efficiency while reducing the risk of overfitting. In addition, its improved structure produces more generalizable features, leading to stronger performance, especially in unseen and cross-domain scenarios.

The Nes2Net consists of an outer layer and several identical nested layers, described as follows:

1) *Outer Layer*: The outer layer of Nes2Net adopts a structure similar to that of Res2Net. The high-dimensional features produced by the speech foundation model are uniformly split into s_1 feature map subsets, denoted by x_i , where $i \in \{1, 2, \dots, s_1\}$. Each feature subset x_i has the same spatial size but contains only $\frac{1}{s_1}$ of the channels of the input feature map. With the exception of x_1 , each x_i is paired with a corresponding nested layer, denoted by $\mathbf{K}_i(\cdot)$. The output of $\mathbf{K}_i(\cdot)$, represented as y_i , is computed as follows:

$$y_i = \begin{cases} x_i & i = 1; \\ \mathbf{K}_i(x_i) & i = 2; \\ \mathbf{K}_i(x_i + y_{i-1}) & 2 < i \leq s_1. \end{cases} \quad (1)$$

where x_i is first added to the output of $\mathbf{K}_{i-1}(\cdot)$, and the resulting feature map is then fed into $\mathbf{K}_i(\cdot)$ for further processing. All y_i features are concatenated along the channel dimension. Due to the combinatorial explosion effect [18], the output features encapsulate a fusion of receptive field characteristics across different scales and frame levels. These features are then pooled along the time axis to convert frame-level features into utterance-level representations, which are subsequently used to compute the final classification score.

It is worth noting that since the outer layer directly processes high-dimensional features from the speech foundation model, the original two convolutional layers (kernel size of 1) used before splitting and after concatenation in Res2Net are removed to improve efficiency.

2) *Nested Layer*: The nested layer acts as the core module responsible for processing the outer layer’s intermediate features, denoted by x'_i , where $i \in \{2, \dots, s_1\}$. Based on Eq. 1, x'_i is defined as:

$$x'_i = \begin{cases} x_i & i = 2; \\ x_i + y_{i-1} & 2 < i \leq s_1. \end{cases} \quad (2)$$

Each nested layer module $\mathbf{K}_i(\cdot)$ is designed to extract multi-scale representations from its input while maintaining computational efficiency. As shown in Fig. 1, the structure of $\mathbf{K}_i(\cdot)$ follows a SE-Res2Net-like design, but its input is the subset feature x'_i from the outer layer of Nes2Net. Specifically, each nested layer consists of the following components:

Convolutional Layers: The input feature map is first processed by a convolutional layer with a kernel size of 1 to extract local features while preserving the spatial dimensions.

Multi-Scale Feature Extraction: To enable multi-scale processing, the input feature map x'_i is equally split into s_2 subsets along the channel dimension, denoted by $x_{i,j}$, where $j \in \{1, 2, \dots, s_2\}$. Each subset undergoes separate transformations through convolutional operations \mathbf{M}_j with varying receptive fields, yielding $y_{i,j}$, formulated as:

$$y_{i,j} = \begin{cases} x_{i,j} & j = 1; \\ \mathbf{M}_j(x_{i,j} + y_{i,j-1}) & 1 < j \leq s_2. \end{cases} \quad (3)$$

These transformed subsets are then concatenated to form the output y_i of the nested layer.

SE Module: To further enhance the feature representations, a Squeeze-and-Excitation (SE) module is integrated into each nested layer. The SE module adaptively recalibrates channel-wise features to emphasize informative features and suppress less relevant ones [41].

Residual Connections: To enhance gradient flow and stabilize training, a residual connection is applied by adding the input of x'_i to its output y_i . This design preserves the original information while incorporating newly learned features.

In summary, the nested layer is lightweight and highly efficient. Its ability to capture multi-scale features ensures that the model maintains robustness and generalization across diverse conditions.

B. Enhanced Nested Res2Net (Nes2Net-X)

While Nes2Net efficiently addresses the high-dimensional feature issue, it relies on an additive combination method within the nested layer, which potentially limits the flexibility and effectiveness of the feature extraction by assigning equal importance to all features. To further enhance the representational capability of Nes2Net, we propose an improved variant, Nes2Net-X, that incorporates concatenation followed by a weighted summation within its nested layers. This design explicitly preserves feature subset individuality before fusion and employs learnable weights to adaptively combine these subsets, offering several advantages:

- **Enhanced Feature Diversity**: By concatenating features across subsets, the network captures a richer set of features, encompassing various aspects of the input data.
- **Learnable Feature Fusion**: The introduction of learnable weights w enables the model to prioritize more informative features, effectively suppressing less relevant ones.

This adaptive mechanism allows the network to focus on the most discriminative features for the task.

- **Improved Gradient Flow:** By combining concatenation with weighted summation, the model facilitates better gradient propagation during training. This helps address potential issues such as vanishing or exploding gradients, leading to more stable and efficient learning.

The Nes2Net-X consists of the following components:

Feature Splitting and Processing: This component is the same as that in the Nes2Net nested layer. The input feature x'_i is equally split into s_2 subsets along the channel dimension, denoted by $x_{i,j}$, where $j \in \{1, 2, \dots, s_2\}$. Each subset $x_{i,j}$ undergoes a convolutional operation to extract feature representations.

Feature Concatenation: The outputs of the convolutional layer are denoted as $z_{i,j}$. In Nes2Net-X, instead of summing the processed features as in the original Nes2Net nested layer, each current subset $x_{i,j}$ is concatenated with the previous output $z_{i,j-1}$ before being processed.

Weighted Sum: The additional dimension created during concatenation is merged back into the original feature space using a ‘weighted sum’ operation. This operation enables the model to dynamically assign importance to each subset, enhancing feature representation. For each subset, the ‘weighted sum’ is applied to the output feature $z_{i,j}$ of the convolutional layer. Let $w_{i,j}$ denote the learnable weights assigned to each concatenated feature. The output $y_{i,j}$ of the ‘weighted sum’ is computed as:

$$y_{i,j} = \sum_{k=1}^s w_{i,j,k} \cdot z_{i,j,k} \quad (4)$$

where s denotes the number of subsets, $w_{i,j,k}$ represents the weight for the k -th subset features $z_{i,j,k}$. The weighted summation allows the model to prioritize more informative features dynamically while suppressing less relevant ones, improving the overall robustness and performance of the nested layer.

These modifications enable Nes2Net-X to retain the strengths of Nes2Net while introducing greater flexibility in feature fusion, ultimately improving performance.

IV. EXPERIMENTAL SETUPS

A. Datasets

TABLE II
AN SUMMARY OF THE DATASETS USED IN OUR EXPERIMENTS.

| Dataset | Spoofing Type | Number of Samples | | |
|--------------------------------------|----------------|-------------------|---------|---------|
| | | Train | Valid | Test |
| CtrSVDD w/o ACESinger bona fide [46] | Singing Voice | 84,404 | 43,625 | 64,734 |
| CtrSVDD w/ ACESinger bona fide [46] | | - | - | 67,579 |
| ASVspooft 2019 [47] | Speech | 25,380 | 24,844 | - |
| ASVspooft 2021 LA [48] | | - | - | 181,566 |
| ASVspooft 2021 DF [48] | | - | - | 611,829 |
| ASVspooft 5 [49] | | 182,357 | 140,950 | 680,774 |
| In-the-Wild [50] | | - | - | 31,779 |
| PartialSpooft [51] | Partial Spooft | 25,380 | 24,844 | 71,237 |

We use five datasets across various scenarios, including singing voice deepfake, fully spoofed speech, adversarial attacks, and partially spoofed speech to evaluate the performance

of the proposed model. Deepfake singing voice detection (SVDD) is a growing area of interest in the research community [46], [52], [53]. Accordingly, we use the Controlled Singing Voice Deepfake Detection (CtrSVDD) dataset [46], [52] as a representative example. Fully spoofed speech is the most studied category. In this work, we include two types of datasets: (1) the ASVspooft series, which comprises ASVspooft 2019 [47], ASVspooft 2021 Logical Access (LA), ASVspooft 2021 Deepfake (DF) [48], and ASVspooft 5 [49] datasets; and (2) the In-the-Wild dataset [50], which reflects real-world usage scenarios. Partially spoofed speech alters only part of an utterance to convey deceptive meaning. This emerging challenge has attracted growing attention. We use the PartialSpooft [51] dataset as a representative benchmark. Table II summarizes the datasets used in this study. Models are trained on the training set and validated on the validation set to select the best checkpoint for testing.

For CtrSVDD [46], we report results on two official test protocols, depending on whether ACESinger bona fide samples are included. A14 is excluded following the dataset’s official guidelines [46]. ASVspooft 2019 [47] is used only for training and validation, while the In-the-Wild [50], ASVspooft 2021 LA and DF [48] datasets are used only for testing. For the recently released ASVspooft 5 dataset [49], we use its train, development, and evaluation partitions for model training, validation, and testing, respectively. For PartialSpooft [51], we follow the standard partitioning into train, development, and evaluation sets.

B. Training Strategies

Each experiment is run three times using different random seeds. We report both the result from the best-performing run and the average performance across all runs. The values of s_1 and s_2 are both set to 8 for Nes2Net and Nes2Net-X. The baseline systems for each dataset are built using SOTA models, and our proposed model adopts similar training strategies. The details are as follows:

CtrSVDD: For the models trained on the CtrSVDD dataset [46], [52], we follow the baseline system from [16]¹. Following the setting in [16], we use a random seed of 42 to ensure reproducibility. Furthermore, due to the inherent stochasticity in deep learning, repeated runs are necessary to obtain reliable average results. We use the AdamW optimizer with batch size 34, an initial learning rate of 1×10^{-6} , and weight decay of 1×10^{-4} . The learning rate is scheduled using cosine annealing with a cycle to a minimum of 1×10^{-9} .

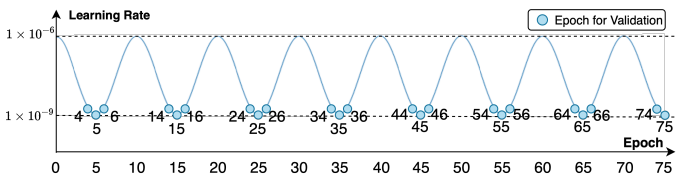


Fig. 2. The cyclic learning rate schedule using cosine annealing, with a minimum value of 1×10^{-9} and a maximum value of 1×10^{-6} .

As shown in Fig. 2, over 75 training epochs, we select checkpoints from the epoch with the minimum learning rate, as

¹<https://github.com/Anmol2059/SVDD2024>

TABLE III

PERFORMANCE IN EER (%) ON THE CTRSVDD EVALUATION SET [46] WITH WAVLM [3] FRONT-END. RESULTS ARE SHOWN AS ‘BEST (MEAN)’ OVER 3 RUNS. PARAMS. AND MMACs REFER TO NUMBER OF PARAMETERS AND MILLION MULTIPLY-ACCUMULATE OPERATIONS, RESPECTIVELY. W/O AND W/ ACE B.F. REFER TO ‘WITHOUT’ AND ‘WITH’ ACESINGER BONA FIDE SAMPLES, RESPECTIVELY. ATTACK-SPECIFIC EERS ARE COMPUTED UNDER THE ‘W/O ACE B.F.’ CONDITION. BEST RESULTS ARE IN **BOLD**; SECOND-BEST ARE UNDERLINED.

| Back-end | Params. | MMACs | EER of Different Attack Types | | | | | Pooled EER | |
|---------------------------|-------------|--------------|-------------------------------|--------------------|--------------------|--------------------|--------------------|--------------------|--------------------|
| | | | A9 | A10 | A11 | A12 | A13 | w/o ACE. B.F. | w/ ACE. B.F. |
| SLS [39] | - | - | - | - | - | - | - | - | 2.59 |
| AASIST [16] | 447k | 707.65 | - | - | - | - | - | - | 2.70 |
| AASIST Light (C=24) | 159k | 91.35 | 1.27 (1.37) | 0.87 (1.00) | 5.44 (5.86) | 4.84 (5.65) | 0.98 (1.05) | 3.95 (4.35) | 3.41 (3.77) |
| AASIST Standard(C=32) | 447k | 707.65 | 1.18 (1.28) | 0.73 (0.86) | 3.63 (3.86) | 5.65 (5.77) | 0.88 (1.00) | 3.30 (3.36) | 2.79 (2.89) |
| AASIST Large(C=40) | 662k | 1,091.28 | <u>1.32</u> (1.37) | 0.87 (0.97) | 3.70 (3.96) | 5.04 (5.63) | 0.96 (1.06) | 3.19 (3.36) | 2.71 (2.94) |
| AASIST XL(C=48) | 835k | 1,555.56 | 1.23 (1.36) | 0.76 (0.92) | 3.40 (4.64) | 4.93 (5.55) | 0.89 (1.06) | 3.12 (3.62) | 2.76 (3.18) |
| AASIST XXL(C=56) | 1,087k | 2,104.57 | 0.96 (1.20) | 0.66 (0.84) | 3.86 (4.15) | 4.83 (5.43) | 0.75 (0.95) | 3.05 (3.43) | 2.65 (2.95) |
| ResNet | 611k | 70.62 | <u>1.18 (1.21)</u> | 0.80 (0.93) | 3.97 (5.06) | <u>4.60 (4.86)</u> | 0.96 (1.03) | 3.11 (3.61) | 2.74 (3.17) |
| Res2Net | 452k | 64.93 | 1.26 (1.37) | 0.83 (0.86) | 3.59 (4.08) | 4.45 (4.80) | 1.08 (1.09) | 3.02 (3.24) | 2.61 (2.78) |
| ECAPA-TDNN (C=128) | 497k | 80.21 | 1.18 (1.39) | 0.67 (0.85) | 4.47 (5.84) | 4.63 (4.96) | 0.87 (1.04) | 3.19 (3.74) | 2.79 (3.30) |
| Proposed Nes2Net | 511k | 58.11 | 1.23 (1.34) | 0.76 (0.81) | 2.40 (2.43) | 5.00 (5.24) | 0.96 (0.99) | 2.53 (2.55) | 2.22 (2.27) |
| Proposed Nes2Net-X | 511k | 91.35 | 1.21 (1.23) | 0.63 (0.76) | 2.09 (2.32) | 4.99 (5.24) | <u>0.83 (0.92)</u> | 2.48 (2.51) | 2.20 (2.24) |

well as its preceding and following epochs, for validation. The best validation result is then used for testing. We use binary focal loss, a generalization of binary cross-entropy loss, with a focusing parameter (γ) of 2 and a positive class weight (α) of 0.25. To standardize input length, each sample is randomly cropped or padded to 4 seconds during training. We adopt the Rawboost ‘parallel: (1)+(2)’ data augmentation strategy [54], as explored in [16]. WavLM is used as the front-end model for this dataset. The pre-trained and implementation of WavLM are obtained from S3PRL².

ASVspoof 2019 & 2021: For the models trained on the ASVspoof 2019 [47] dataset, we follow the baseline system proposed in [15]³. Audio data are cropped or concatenated to create segments of approximately 4 seconds in duration (64,600 samples). We use the Adam optimizer [55] with a weight decay of 1×10^{-4} . To reproduce the AASIST baseline [15], we reduce the original batch size from 14 to 8 due to GPU memory constraints, and halve the learning rate from 1×10^{-6} to 5×10^{-7} . For Nes2Net, benefiting from its lower GPU memory consumption, we use a batch size of 12 with a learning rate of 2.5×10^{-7} . The loss function used is weighted Cross Entropy. Following [15], we apply Rawboost augmentations [54], specifically ‘series: (1+2+3)’ (Algo4) and ‘series: (1+2)’ (Algo5), for AASIST baselines. For the proposed Nes2Net-X, only the former augmentation is applied. All models are trained for 100 epochs and the best checkpoint on the validation set is used for testing on the ASVspoof 2021 [48] and In-the-Wild [50] datasets.

ASVspoof 5: Both our baseline AASIST and the proposed Nes2Net-X models are trained using settings similar to those used for AASIST in the ASVspoof 2019 corpus. However, several differences apply. The final learning rate is set to 1×10^{-7} , we apply data augmentation using MUSAN [56] and RIR [57], and training is stopped if there is no improvement on the development set for 5 consecutive epochs. Following the ASVspoof 5 challenge guidelines [49], we use WavLM [3] as the front-end, replacing wav2vec 2.0 [1] used in our ASVspoof 2019 experiments.

PartialSpoof: For models trained on the PartialSpoof [51], we follow the baseline systems described in [51], [58]⁴. Specifically, we use wav2vec 2.0 as the front-end, the MSE for P2SGrad [59] as the loss function, and Adam [55] as the optimizer. Following [58], the batch size is set to 2, and a learning rate of 2.5×10^{-6} is adopted for the baseline systems. For the proposed Nes2Net and Nes2Net-X, the learning rate is set to 1×10^{-5} . The pooling layer used for the proposed Nes2Net and Nes2Net-X is the Attentive Statistics Pooling [42], and the reduction ratio of SE module is set to 8. Training is terminated if no improvement is observed on the development set for 20 consecutive epochs. The epoch yielding the best performance on the development set is used for testing.

V. RESULTS AND ANALYSIS

In this section, we provide an extensive validation of the proposed Nes2Net across a wide range of datasets. We begin by exploring the design motivation and development path of Nes2Net using the CtrSVDD dataset. These insights are further validated on ASVspoof 2021, ASVspoof 5, In-the-Wild, and PartialSpoof datasets. Our experimental setup covers a broad spectrum of scenarios to ensure comprehensive evaluation, including singing voice deepfakes, fully spoofed speech, adversarial attacks, partially spoofed speech, and real-world deepfake cases.

A. Studies on the CtrSVDD dataset

We conduct experiments on the CtrSVDD dataset [46], following two testing protocols: one including ACESinger bona fide samples and the other excluding them [38]. While results for both protocols are reported in Table III, our primary analysis focuses on the scenario ‘**without ACESinger bona fide (w/o ACE. B.F.)**’, as recommended by the dataset creators.

First, we reproduce the SOTA baseline system, AASIST Standard (C=32), achieving an EER of 2.79%, closely matching the originally reported 2.70% [16]. Under the ‘w/o ACE B.F.’ condition, the best run achieves an EER of 3.30%, with

²<https://github.com/s3prl/s3prl>

³https://github.com/TakHemlata/SSL_Anti-spoofing

⁴<https://github.com/nii-yamagishilab/PartialSpoof>

TABLE IV

PERFORMANCE IN EER (%) ON THE CTRSVDD EVALUATION SET [46], COMPARING THE PROPOSED NES2NET WITH RES2NET AND ITS VARIOUS VARIANTS. THE RESULTS ARE REPORTED AS THE FORMAT OF ‘BEST (MEAN)’ ACROSS 3 RUNS, E.G., 3.02 (3.24) IN THE FIRST ROW, OR AS THE RESULT OF A SINGLE EXPERIMENT, E.G., 3.21 IN THE SECOND ROW. ‘B’ AND ‘S’ REPRESENT THE NUMBER OF BLOCKS AND SCALE OF RES2NET, RESPECTIVELY.

| Back-end | Dimensionality Reduction Layer | Reduced Dimension D | Params. | MMACs | Pooled EER | | Remarks |
|-------------------------------|--------------------------------|-----------------------|---------|--------|--------------------|--------------------|--|
| | | | | | w/o ACE. B.F. | w/ ACE. B.F. | |
| Res2Net ($b=4, s=4$) | ✓ | 128 | 452k | 64.93 | 3.02 (3.24) | 2.61 (2.78) | |
| Res2Net ($b=4, s=16$) | ✓ | 128 | 427k | 59.95 | 3.21 | 2.80 | ■ increase scale s |
| Res2Net ($b=4, s=64$) | ✓ | 128 | 419k | 58.28 | 3.15 | 2.74 | |
| Res2Net ($b=4, s=128$) | ✓ | 128 | 417k | 57.98 | 3.26 | 2.88 | |
| Res2Net ($b=4, s=4$) | ✓ | 64 | 180k | 23.25 | 4.32 | 3.76 | ■ change D |
| Res2Net ($b=4, s=4$) | ✓ | 256 | 1,273k | 202.91 | 3.83 | 3.38 | |
| Res2Net-woDR ($b=1, s=4$) | × | - | 861k | 119.15 | 4.15 | 3.62 | |
| Res2Net-woDR ($b=1, s=8$) | × | - | 615k | 70.12 | 4.23 | 3.71 | |
| Res2Net-woDR ($b=1, s=16$) | × | - | 456k | 38.24 | 3.82 | 3.35 | ■ remove dimensionality reduction layer and increase scale s |
| Res2Net-woDR ($b=1, s=32$) | × | - | 367k | 20.45 | 2.98 (3.45) | 2.56 (3.02) | |
| Res2Net-woDR ($b=1, s=64$) | × | - | 320k | 11.10 | 2.73 (2.97) | 2.42 (2.61) | |
| Res2Net-woDR ($b=1, s=128$) | × | - | 296k | 6.31 | 3.29 | 2.88 | |
| Res2Net-woDR ($b=1, s=256$) | × | - | 284k | 3.88 | 3.57 | 3.13 | |
| Res2Net-woDR ($b=2, s=64$) | × | - | 637k | 21.78 | 3.20 | 2.82 | ■ increase depth |
| Res2Net-woDR ($b=4, s=64$) | × | - | 1,270k | 43.15 | 3.09 (3.18) | 2.73 (2.83) | |
| Proposed Nes2Net | × | - | 511k | 58.11 | 2.53 (2.55) | 2.22 (2.27) | ■ proposed nested design |
| Proposed Nes2Net-X | × | - | 511k | 91.35 | 2.48 (2.51) | 2.20 (2.24) | |

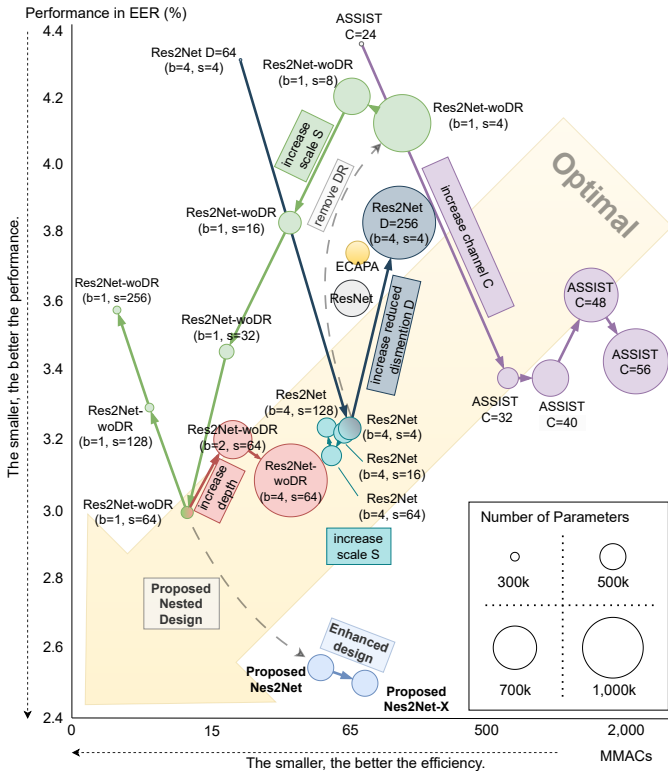


Fig. 3. Visualization of Table III and IV, highlighting our exploration of Res2Net and the roadmap of architectural changes leading to Nes2Net.

an average of 3.36% across three runs. Further experiments show that scaling up the AASIST model does not improve EER, possibly due to parameter redundancy.

We additionally evaluate several widely-used baseline systems, including ResNet [19], Res2Net [18], and ECAPA-TDNN [34]. ECAPA-TDNN and ResNet achieve EERs of 3.74% and 3.61%, respectively, which are slightly worse than that of AASIST. In contrast, Res2Net benefits from the advantages of multi-scale feature extraction, delivering the best average performance among the baseline systems

with an EER of 3.24%. Our proposed Nes2Net outperforms all baseline systems, achieving an EER of 2.55% with the lowest computational cost. Furthermore, the enhanced version, Nes2Net-X, further improves the performance to 2.51% EER, marking the best single-model performance reported to date. Compared to Res2Net, ResNet, ECAPA-TDNN, and SOTA AASIST ($C = 32$), Nes2Net-X achieves EER reductions of 23%, 30%, 33%, and 25%, respectively.

We also analyze performance across different synthetic attack types using the ‘w/o ACE B.F.’ protocol. Except for the A12 track, our model consistently achieves either the best or second-best performance, demonstrating strong generalization and robustness. Notably, the A12 track—based on Singing Voice Synthesis (SVS)—proves particularly challenging, showing higher EER across all models and highlighting a potential area for future improvement.

We observe that performance trends are consistent across both conditions—with and without ACESinger bona fide samples. Moreover, the EER is lower when ACESinger bona fide samples are included. This indicates that, even though ACESinger bona fide samples are considered out-of-domain, the trained models exhibit strong generalization capabilities and are able to classify these samples accurately.

B. The Roadmap of the Nes2Net

In this section, we introduce the roadmap from Res2Net to the proposed Nes2Net, with detailed results summarized in Table IV. To aid interpretation, we visualize the number of parameters, MACs, and EER. These are represented in Fig. 3 by circle size, the horizontal axis, and the vertical axis, respectively. In the following, we provide detailed analyses:

Investigating Res2Net: Among the baselines in Table III, the Res2Net-based back-end outperforms ResNet, AASIST, and ECAPA-TDNN on the CtrSVDD dataset. Therefore, we select it as the reference baseline for further investigation. First, we experiment with adjusting the scale s of Res2Net. We observe that as s increases, the number of split groups

increases linearly; however, the performance shows no significant improvement (depicted as the teal blue line in Fig. 3). This may be because adding too many split groups dilutes the feature representation, leading to redundancy and limited benefit.

Next, we explore varying the dimensionality of the output features from the DR layer (referred to as Reduced Dimension D , depicted as the steel gray line in Fig. 3). Reducing D to 64 significantly lowers model size and MACs compared to the default $D = 128$, but leads to substantial performance degradation, increasing EER from 3.02% to 4.32%. Conversely, increasing D to 256 results in a much larger model size and MACs but still leads to worse performance than $D = 128$. This may be because a larger D introduces over-parameterization and noise. This likely explains why $D = 128$ is commonly adopted in SOTA models [15], [16].

Removal of DR Layer: Foundation models often incorporate a DR layer in their back-end architecture to compress high-dimensional features into lower-dimensional representations, facilitating downstream tasks. For instance, models like wav2vec 2.0-AASIST [15] utilize such a layer alongside task-specific classifiers (e.g., AASIST, ResNet). However, as discussed in Section II-E, this projection layer consumes a substantial portion of the back-end model’s parameters and MACs while potentially causing information loss.

To explore whether bypassing this layer preserves more task-relevant information, we propose a new back-end model: **ResNet without Dimensionality Reduction (ResNet-woDR)**. By directly processing high-dimensional features, ResNet-woDR simplifies the architecture and focuses on the raw features extracted by the speech foundation model. The naming emphasizes the absence of a DR layer, differentiating it from traditional approaches.

We further evaluate the performance of ResNet-woDR with different scales s (depicted as the green line in Fig. 3). The best performance is observed with $s = 64$, achieving an EER of 2.73%, which surpasses the best Res2Net baseline. Increasing s beyond this point leads to a decline in performance, likely due to the following factors:

- **Feature Dilution.** A large s excessively fragments feature representations, weakening their expressiveness and resulting in diluted, less informative features [18].
- **Redundant Transformations.** An overly large s introduces unnecessary feature transformations, leading to overfitting and reduced generalization [43].
- **Restricted Feature Interaction.** Since channels are unordered, distant groups may still contain correlated information. In this case, the additional convolutional layers introduced by splitting limit their interactions, weakening the model’s ability to capture complex patterns.

Based on the optimal s , we increase the number of blocks b to deepen the model (depicted as the light pink line in Fig. 3). However, no further performance improvement is observed. This may be because the deeper architecture does not effectively leverage the additional parameters, resulting in diminishing performance gains. It may also increase the risk of overfitting.

The Novel Nested Design: Prior experiments demonstrate that removing the DR layer enhances the performance of Res2Net. We believe that directly extracting information from high-dimensional speech foundation model features avoids the information loss introduced by DR. Our experiments with variations in scale, depth, and dimensionality show that an EER of 2.73% represents the performance bottleneck for this design.

Compared to ResNet-woDR, the proposed Nes2Net adopts a novel nested design that enhances flexibility and significantly boosts the model’s representational capacity. Processing larger feature subsets in the outer layer facilitates better interactions across channels within each nested layer. Furthermore, the integrated local cross-channel attention mechanism enhances feature selection while mitigating redundancy, addressing limitations in prior designs. This architectural refinement overcomes the performance limitations observed in the original Res2Net design. As a result, Nes2Net and its enhanced variant Nes2Net-X surpass the earlier performance bottleneck, achieving average EERs of 2.55% and 2.51%, respectively.

C. Activation Function

TABLE V
PERFORMANCE IN EER (%) ON THE CTRSVDD EVAL SET [46] FOR COMPARING WITH PROPOSED NES2NET WITH DIFFERENT ACTIVATION FUNCTIONS. THE RESULTS ARE REPORTED AS THE FORMAT OF ‘BEST (MEAN)’ ACROSS 3 RUNS.

| Front-end | Back-end | Activation Function | Pooled EER | |
|-----------|-----------|---------------------|----------------------|----------------------|
| | | | w/o ACE. B.F. | w/ ACE. B.F. |
| WavLM | Nes2Net-X | ReLU [60] | 2.48 (2.51) | 2.20 (2.24) |
| | | GELU [61] | 2.52 (2.56) | 2.22 (2.26) |
| | | SiLU [62] | 2.52 (2.55) | 2.22 (2.25) |
| | | SELU [63] | 2.28 (2.69) | 2.02 (2.37) |

Activation functions like Rectified Linear Unit (ReLU) [60], Scaled Exponential Linear Units (SELU) [63], Gaussian Error Linear Units (GELU) [61], and Sigmoid Linear Unit (SiLU) [62] address common deep learning challenges, such as vanishing gradients. By introducing diverse characteristics like improved gradient flow, self-normalization, or smooth transitions, these functions aim to enhance model convergence, stability, and overall performance in complex scenarios.

We experiment with replacing the default ReLU activation function with several alternatives and present the results in Table V. GELU and SiLU do not yield any performance improvements over ReLU. Although SELU achieves better performance in one of the three runs, its average performance does not improve. This suggests higher variance across runs. This suggests that SELU does not offer a consistent advantage over ReLU in our experimental setup. Therefore, we retain ReLU as the default activation function in our model.

D. Studies on the ASVspoof 2021 dataset

The ASVspoof series datasets are widely used as benchmarks for advancing research in detecting spoofed speech [47], [48]. Following standard protocol, we train our models on ASVspoof 2019 [47] and evaluate them on ASVspoof 2021

TABLE VI

PERFORMANCE IN EER (%) ON THE ASVspoof 2021 LA AND DF. THE RESULTS ARE REPORTED IN THE FORMAT OF ‘BEST (MEAN)’. CKPT AVG. REFERS TO THE NUMBER OF CHECKPOINTS AVERAGED. ‘RE-IMP’ DENOTES RE-IMPLEMENTATION CONDUCTED BY US. ‘ALGO4’ AND ‘ALGOS’ REPRESENT RAWBOOST SERIES AUGMENTATIONS: ‘(1+2+3)’ AND ‘(1+2)’ [54], RESPECTIVELY. PARAMETERS THAT ARE UNDERLINED ARE CALCULATED BY US. ‘-’ REPRESENTS UNKNOWN. ‘N/A’ INDICATES THAT THE SYSTEM DOES NOT USE THE AVERAGE CHECKPOINTS METHOD.

| Remark | Front-end | Back-end Model | Back-end Parameters | CKPT Avg. | ASVspoof 2021 | |
|--------|-------------|---------------------|----------------------|-----------|--------------------|--------------------|
| | | | | | LA | DF |
| 2022 | wav2vec 2.0 | FIR-NB [64] | - | - | 3.54 | 6.18 |
| 2022 | wav2vec 2.0 | FIR-WB [64] | - | - | 7.08 | 4.98 |
| 2022 | wav2vec 2.0 | LGf [65] | - | - | 9.66 | 4.75 |
| 2023 | wav2vec 2.0 | Conformer [66] | 2,51k ⁵ | - | 1.38 | 2.27 |
| 2024 | wav2vec 2.0 | Ensembling [67] | - | - | 2.32 (4.48) | 5.60 (8.74) |
| 2024 | WavLM | ASP+MLP [68] | <u>1,051k</u> | - | 3.31 | 4.47 |
| 2024 | wav2vec 2.0 | SLIM [14] | - | - | - | 4.4 |
| 2024 | WavLM | AttM-LSTM [31] | 936k ⁶ | N/A | 3.50 | 3.19 |
| 2024 | wav2vec 2.0 | FTDKD [69] | - | - | 2.96 | 2.82 |
| 2024 | wav2vec 2.0 | AASIST2 [70] | - | - | 1.61 | 2.77 |
| 2024 | wav2vec 2.0 | MFA [71] | - | - | 5.08 | 2.56 |
| 2024 | wav2vec 2.0 | MoE [72] | - | - | 2.96 | 2.54 |
| 2024 | wav2vec 2.0 | OCKD [73] | - | - | 0.90 | 2.27 |
| 2024 | wav2vec 2.0 | TCM [33] | 2,383k ⁷ | 5 | 1.03 | 2.06 |
| 2024 | wav2vec 2.0 | SLS [35] | 23,399k ⁸ | - | 2.87 (3.88) | 1.92 (2.09) |
| 2025 | wav2vec 2.0 | LSR+LSA [74] | - | - | 1.19 | 2.43 |
| 2025 | wav2vec 2.0 | LSR+LSA [74] * | - | - | 1.05 * | 1.86 * |
| 2025 | wav2vec 2.0 | conf. ensemble [75] | - | - | - | 2.03 |
| 2025 | wav2vec 2.0 | WaveSpec [76] | - | - | - | 1.90 |
| 2025 | wav2vec 2.0 | Mamba [17] | 1,937k ⁹ | 5 | 0.93 | 1.88 |
| 2022 | wav2vec 2.0 | AASIST [15] | 447k ¹⁰ | N/A | 0.82 (1.00) | 2.85 (3.69) |
| re-imp | wav2vec 2.0 | AASIST (algo4) | 447k | N/A | 1.13 (1.36) | 3.37 (4.09) |
| re-imp | wav2vec 2.0 | AASIST (algo5) | 447k | N/A | 0.93 (1.40) | 3.56 (5.07) |
| | wav2vec 2.0 | Nes2Net-X | 511k | N/A | 1.73 (1.95) | 1.65 (1.91) |
| Ours | wav2vec 2.0 | Nes2Net-X | 511k | 3 | 1.66 (1.87) | 1.54 (1.98) |
| | wav2vec 2.0 | Nes2Net-X | 511k | 5 | 1.88 (2.00) | 1.49 (1.78) |

*: with extra data augmentation.

Logical Access (LA) and Deepfake (DF) tasks [48]. The LA task focuses on detecting synthetic and voice-converted speech transmitted over telephony systems, introducing challenges related to channel effects and transmission variability. In contrast, the DF task targets detecting manipulated, compressed speech data commonly found on online platforms. This reflects real-world scenarios where deepfake audio circulates, making the DF task a valuable benchmark for evaluating deepfake detection systems.

The results in Table VI show that for the LA track, our model achieves the best performance of 1.66% EER, comparable to SOTA systems. For the DF track, which more closely reflects real-world scenarios as discussed earlier, the baseline system AASIST [15] achieves a 2.85% EER, remaining competitive with current SOTA systems. The SLS [35] and TCM [33] models achieve EERs close to 2%, demonstrating strong performance at the SOTA level. The Mamba-based [17] model further improves results, reducing the EER to 1.88%. Notably, our proposed Nes2Net-X achieves the best performance among all compared systems, with an EER of 1.65%.

Inspired by prior works [17], [33], we further experiment by averaging the weights of the top-performing validation checkpoints to produce an improved model. This approach further

improves the performance of the DF task to an EER of 1.49%, which, to the best of our knowledge, is the best performance reported to date. Furthermore, compared to Mamba [17], our model achieves this performance with approximately 74% fewer parameters, demonstrating superior efficiency.

The analysis above summarizes overall performance on the DF test set. The DF dataset also provides detailed labels for vocoder types and compression conditions, enabling more fine-grained analysis. To further evaluate performance, we compare the SOTA models—Mamba, SLS, TCM, and AASIST—with our proposed Nes2Net-X across these sub-tracks. The results are presented in Table VII. To improve readability and make the extensive numerical data easier to interpret, we also visualize the table’s results in Fig. 4.

For traditional vocoders, all models perform well, with most EERs below 2%. Notably, our proposed Nes2Net-X achieves exceptional results, consistently yielding EERs under 1% across all conditions except C2. This demonstrates the strong stability of Nes2Net-X when handling unseen and relatively simple scenarios. In contrast, for neural autoregressive vocoders, all models experience a noticeable drop in performance, with EER reaching up to 5.96%. This indicates the greater challenge posed by the sequential and dynamic nature of autoregressive vocoders, which introduce higher variability in synthesis. Nevertheless, Nes2Net-X maintains a clear advantage over the competing models, demonstrating its robustness in handling these complex synthesis conditions.

From the perspective of compression conditions, the differences in model performance are less pronounced compared to the variations observed across vocoder types. Nes2Net-X consistently achieves the lowest EERs across all compression conditions, regardless of the level of distortion introduced by compression. This consistency highlights the model’s adaptability and strong generalization ability across different levels of compressions.

Overall, these findings demonstrate that Nes2Net-X is not only highly effective across diverse vocoder types, but also maintains superior performance under varying compression conditions. This robustness underscores the model’s capability to handle both compression diversity and complex synthesis challenges, making it a reliable solution for deepfake audio detection across a wide range of scenarios.

E. The results on the In-the-Wild dataset

The In-the-Wild dataset [50] is a collection of deepfake videos sourced from the internet. Unlike controlled datasets, it captures the diverse and unpredictable nature of real-world scenarios. This diversity is essential for developing and evaluating deepfake detection models, as it challenges them to generalize effectively across a wide range of conditions.

In addition, unlike many other datasets that rely on self-generated fake audio, this dataset is collected from publicly available video and audio files explicitly labeled as audio deepfakes [50]. To account for the potential presence of partial spoofing, we evaluate our proposed Nes2Net-X using the entire duration of each test sample instead of restricting it to the first 4 seconds, as the latter approach risks missing partially spoofed segments.

⁵<https://github.com/ErosRos/conformer-based-classifier-for-anti-spoofing>

⁶https://github.com/pandarialTJU/AttM_INTERSPEECH24

⁷https://github.com/ductuantruong/tcm_add

⁸<https://github.com/QiShanZhang/SLSforASVspoof-2021-DF>

⁹<https://github.com/swagshaw/XLSR-Mamba>

¹⁰https://github.com/TakHemlata/SSL_Anti-spoofing

TABLE VII

PERFORMANCE IN EER (%) FOR DIFFERENT TYPES OF VOCODERS AND COMPRESSION CONDITIONS ON THE ASVspOOF 2021 DF TEST SET. THE FIVE EER VALUES FOR EACH SUB-ITEM, FROM LEFT TO RIGHT, CORRESPOND TO NES2NET-X, MAMBA [17], SLS [35], TCM [33], AND AASIST [15]. THE BEST PERFORMANCE IS REPORTED IN BOLD FONTS, AND THE SECOND-BEST IS UNDERLINED.

| | Traditional Vocoder | Wav Concatenation | Neural Autoreg. | Neural Non-autoreg. | Unknown | Pooled EER |
|-------------|-----------------------------------|-----------------------------------|---|-----------------------------------|-----------------------------------|----------------------------------|
| C1 - | 0.36/0.78/1.21/0.95/1.22 | 0.76/0.76/0.80/0.76/2.28 | 2.70/3.88/3.12/3.89/3.45 | 0.52/0.87/0.68/0.95/1.56 | 1.64/1.63/1.23/1.73/1.99 | 1.47/1.89/1.72/2.23/2.34 |
| C2 Low mp3 | 1.48/ 0.94 /1.94/1.67/2.72 | 2.96/2.20/ 2.16 /2.56/5.84 | 2.89/3.23/ 2.71 /3.59/5.96 | 1.23/0.86/ 0.78 /1.32/3.33 | 2.54/1.69/ 1.65 /1.93/4.30 | 1.75/1.84/2.02/2.11/4.30 |
| C3 High mp3 | 0.44/0.88 /1.39/0.96/1.83 | 1.13/1.49/1.17/1.45/3.35 | 2.47 /3.35/2.91/3.70/3.79 | 0.44 /0.87/0.69/0.88/2.02 | 2.29/1.85/ 1.34 /1.67/2.65 | 1.32/1.85/1.59/1.95/2.64 |
| C4 Low m4a | 0.44/0.95 /1.48/1.22/1.57 | 1.15/ 0.85 /1.24/1.67/2.09 | 2.79 /3.39/ 2.79 /3.40/3.75 | 0.54 /0.96/0.70/1.22/1.65 | 1.32/1.22/ 1.14 /1.41/2.10 | 1.40/1.92/1.74/2.01/2.37 |
| C5 High m4a | 0.45/0.80 /1.34/0.98/1.16 | 0.62 /0.76/0.71/0.76/2.10 | 2.77 /3.48/2.96/3.73/3.39 | 0.56 /0.90/0.64/1.07/1.34 | 1.88/1.70/ 1.34 /1.43/1.87 | 1.59/2.05/1.79/1.96/2.14 |
| C6 Low ogg | 0.69/1.13 /2.14/1.44/2.35 | 0.80/0.97/0.91/0.91/2.23 | 1.92 /2.80/2.44/2.79/3.67 | 0.48 /0.78/0.61/0.84/1.62 | 1.05/1.14/ 1.00 /1.01/2.23 | 1.09/1.61/1.88/1.87/2.58 |
| C7 High ogg | 0.70/1.13 /1.52/1.35/1.57 | 0.62 /0.80/0.71/0.80/1.50 | 2.05 /2.84/2.26/2.66/2.92 | 0.43 /0.65/0.52/0.74/1.00 | 1.34/1.05/ 0.96/0.96 /1.27 | 1.35/1.61/1.57/1.74/1.92 |
| C8 mp3→m4a | 0.95/1.26 /2.28/1.74/3.01 | 1.52/ 0.97 /1.08/1.08/2.96 | 2.22 /3.01/2.31/2.96/4.49 | 0.61/ 0.57 /0.65/0.95/2.05 | 1.61/1.18/ 1.09 /1.18/2.66 | 1.48/1.65/1.92/1.97/3.31 |
| C9 ogg→m4a | 0.70/1.26 /2.15/1.49/2.28 | 0.88/0.97/0.99/0.88/2.52 | 1.92 /3.01/2.57/2.88/3.76 | 0.52 /0.70/0.65/0.78/1.57 | 0.96 /1.09/1.09/1.05/2.14 | 1.13/1.79/2.04/1.88/2.75 |
| Pooled EER | 0.72/1.14 /1.88/1.40/2.15 | 1.10/ 1.05 /1.07/1.14/2.85 | 2.70 /3.32/2.86/3.40/4.05 | 0.63 /0.80/0.69/0.94/1.84 | 1.86/1.43/ 1.23 /1.38/2.45 | 1.49 /1.88/1.92/2.06/2.85 |

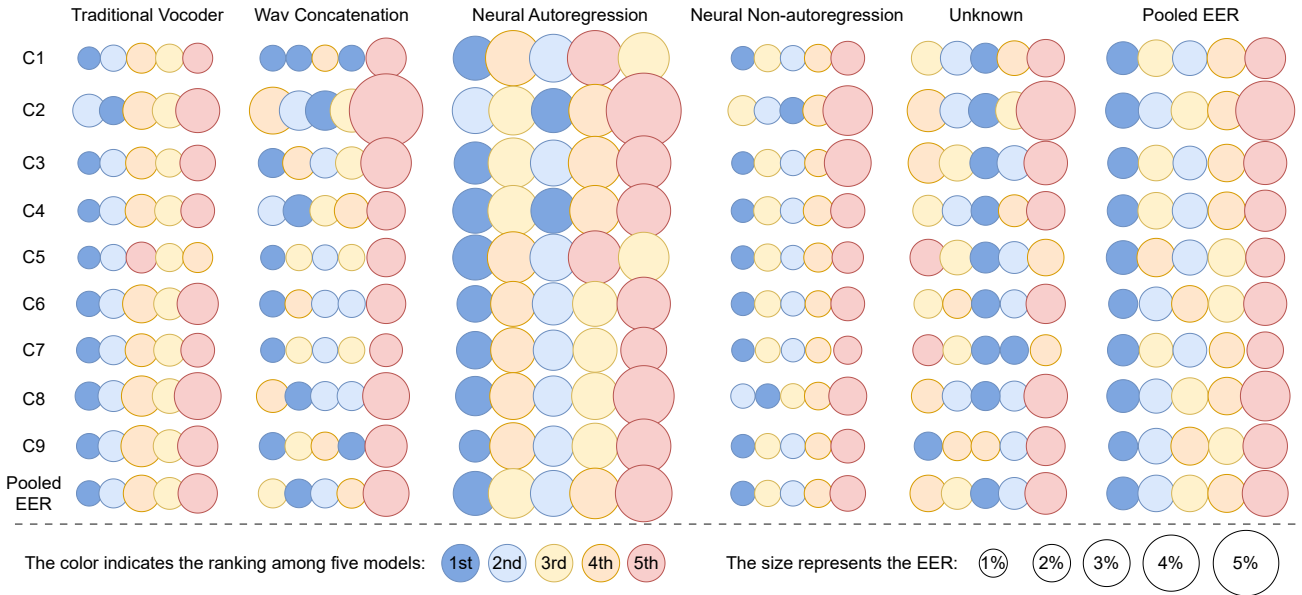


Fig. 4. Visualization of the EER (%) across various vocoders and compression conditions on the ASVspOOF 2021 DF test set. Each EER value is shown as a colored circle, where the size indicates the EER value, and the color represents the performance ranking among the five models: blue (best) to light red (worst). The five EER values for each sub-item, from left to right, correspond to the proposed Nes2Net-X, Mamba [17], SLS [35], TCM [33], and AASIST [15].

TABLE VIII

PERFORMANCE IN EER (%) ON THE IN-THE-WILD [50] DATASET. OUR RESULT IS REPORTED AS THE FORMAT OF ‘BEST (MEAN)’ ACROSS 3 RUNS.

| Front-end | Year | Back-end | EER |
|-------------|------|---------------------------|--------------------|
| wav2vec 2.0 | 2022 | AASIST [15] | 10.46 |
| | 2024 | SLIM [14] | 12.5 |
| | 2024 | MoE [72] | 9.17 |
| | 2024 | Conformer [66] | 8.42 |
| | 2024 | TCM [33] | 7.79 |
| | 2024 | OCKD [73] | 7.68 |
| | 2024 | SLS [35] | 7.46 |
| | 2024 | Pascu et al. [77] | 7.2 |
| | 2025 | Mamba [17] | 6.71 |
| | 2025 | WaveSpec [76] | 6.58 |
| | 2025 | LSR+LSA [74] | 5.92 |
| | 2025 | LSR+LSA [74] * | 5.54 * |
| | - | Proposed Nes2Net-X | 5.52 (6.60) |

*: with extra data augmentation.

The testing results, alongside SOTA models, are reported in Table VIII. We find that the overall performance trends are consistent with those seen on the ASVspOOF 2021 DF dataset. However, EERs on the In-the-Wild dataset are generally higher than those on the DF dataset, reflecting greater complexity

and variability in real-world scenarios. Notably, the proposed Nes2Net-X outperforms all SOTA models, achieving the lowest EER of 5.52% on this challenging dataset.

F. The results on the ASVspOOF 5 dataset

The ASVspOOF 5 dataset represents the most recent edition in the ASVspOOF series. Unlike earlier versions, it introduces adversarial attacks and is crowdsourced under various acoustic conditions [49]. As it is newly released, there are currently no existing systems available for a fair comparison. Therefore, using the WavLM front-end, we implement the AASIST system as a baseline and compare it with our proposed Nes2Net-X model. Based the evaluation protocol in [37], we assess performance using three metrics: Cost of Log-Likelihood Ratio (CLLR), minimum Detection Cost Function (minDCF), and EER, and present the results in Table X. We observe that the Nes2Net-X back-end model results in only a slight increase in the number of parameters compared to AASIST, while significantly reducing MMACs. Moreover, across all three evaluation metrics, the Nes2Net-X back-end improves performance by 10.9%.

TABLE IX

THE PERFORMANCE IN EER (%) ON THE ASVspoof 2021 LA, DF [48], AND IN-THE-WILD [50] DATASETS. THE RESULTS ARE REPORTED AS THE FORMAT OF ‘BEST (MEAN)’ ACROSS 3 RUNS. ‘w/ AUG.’ AND ‘w/o AUG.’ INDICATE WHETHER EVALUATION WITH AUGMENTATIONS ON THE VALIDATION SET IS USED TO SELECT THE BEST CHECKPOINT FOR TESTING. CKPT AVG. REFERS TO THE NUMBER OF CHECKPOINTS AVERAGED.

| Back-end | Train Set | CKPT Avg. | w/ Aug. | | | w/o Aug. | | |
|-----------|------------------|-----------|-------------|-------------|------------------|-------------|-------------|------------------|
| | | | 21LA [48] | 21DF [48] | In-the-Wild [50] | 21LA [48] | 21DF [48] | In-the-Wild [50] |
| Nes2Net-X | ASVspoof 19 [47] | N/A | 1.63 (1.79) | 1.84 (2.03) | 5.56 (6.61) | 1.73 (1.95) | 1.65 (1.91) | 5.73 (6.83) |
| | | 3 | 1.70 (1.80) | 1.88 (1.98) | 5.15 (6.31) | 1.66 (1.87) | 1.54 (1.98) | 5.59 (6.90) |
| | | 5 | 1.67 (1.78) | 1.80 (1.91) | 5.28 (6.31) | 1.88 (2.00) | 1.49 (1.78) | 5.52 (6.60) |

TABLE X

A COMPARISON BETWEEN THE PROPOSED NES2NET AND THE AASIST BASELINE SYSTEM ON THE ASVspoof 5 DATASET [49]. ‘PARAMS.’ AND ‘MMACS’ REFER TO THE NUMBER OF PARAMETERS AND THE NUMBER OF MILLION MULTIPLY-ACCUMULATE OPERATIONS, RESPECTIVELY. ‘AVG.’ INDICATES THE AVERAGE RELATIVE PERFORMANCE IMPROVEMENT ACROSS ALL THREE EVALUATION METRICS.

| Back-end | | Performance | | | | |
|-----------|-------------|--------------|---------------|---------------|-------------|--------------|
| Model | Params.↓ | MMACs↓ | CLLR↓ | minDCF↓ | EER↓ | Avg. |
| AASIST | 447k | 707.65 | 0.9587 | 0.1645 | 6.08 | Benchmark |
| Nes2Net-X | 511k | 91.35 | 0.7344 | 0.1535 | 5.92 | 10.9% |

G. The results on the PartialSpoof dataset

TABLE XI

PERFORMANCE IN EER(%) ON THE PARTIALSPOOF [51] DATASET. THE RESULTS ARE REPORTED AS THE FORMAT OF ‘BEST (MEAN)’ ACROSS 3 RUNS. † INDICATES RESULTS OBTAINED FROM OUR IMPLEMENTATION.

| Front-end | Year | Back-end | PartialSpoof [51] | |
|-------------|------|-----------------|--------------------|----------------------|
| | | | Dev | Eval |
| wav2vec 2.0 | 2024 | gMLP [51] | 0.35 | 0.64 |
| | - | gMLP† | 0.39 (0.43) | 0.72 (0.80) |
| | 2024 | 1D Res2Net [58] | 0.35 | 0.73 |
| | - | 1D Res2Net† | 0.35 (0.38) | 0.73 (0.79) |
| | - | SE ResNet† | 0.31 (0.50) | 0.77 (0.78) |
| | - | Nes2Net | 0.24 (0.36) | 0.53 (0.68) |
| | - | Nes2Net-X | 0.20 (0.33) | 0.57 (0.64) |

Partially manipulating a sentence can significantly alter its intended meaning [58]. When such manipulations occur in small regions, existing models—trained on fully spoofed speech and relying on pooling functions—struggle to detect these subtle changes. Consequently, there is growing interest in the detection of partially spoofed speech [51], [58], [78].

To evaluate the performance of our proposed model across different datasets and spoofing tasks, we conduct experiments on the PartialSpoof dataset [51]. The results are presented in Table XI. First, we reproduce the performance of two SOTA models, achieving results comparable to those reported in their original papers [51], [58]. Additionally, we evaluate SE ResNet, which demonstrated performance similar to the other baselines. In contrast, our proposed Nes2Net and Nes2Net-X significantly outperform all three baselines, achieving relative performance improvements of 36.6% and 25.6%, respectively.

H. Should We Use Augmentation During Validation?

In all previous experiments, the datasets are split into three non-overlapping subsets: training, validation (or development),

and test sets. The validation set is used to select the best-performing checkpoints for final evaluation on the test set. The training set typically applies data augmentation to enhance model performance and generalization. However, the use of augmentation during validation remains inconsistent across prior studies. For instance, wav2vec 2.0-AASIST [15] applies the same augmentation strategy to both training and validation sets. In contrast, WavLM-AASIST [16] does not use augmentation on the validation set, aligning with common practices in speaker verification research [34], [79], [80].

In this section, we compare these two approaches and report the results in Table IX. We observe that applying the same augmentation to the validation set as in the training set leads to worse performance on ASVspoof 2021 DF [48], but better results on In-the-Wild [50]. When no augmentation is applied to the validation set, the opposite trend is observed.

From the outcome of the above study, we believe that in cases where robustness to certain variations (e.g., noise, compression, or distortions) is important, applying augmentation during validation provides insights into how well the model handles such conditions. As a result, the selected checkpoints from this approach may generalize better to these variations. Further investigation into this topic may yield deeper insights for future work.

VI. CONCLUSION

In this work, we propose Nested Res2Net (Nes2Net) and its enhanced variant, Nes2Net-X, as lightweight and dimensionality reduction (DR) layer-free back-end architectures designed for speech anti-spoofing in the foundation model era. Unlike conventional approaches that rely on a DR layer to bridge the mismatch between high-dimensional features and downstream classifiers, our proposed architectures directly process these rich representations. This not only eliminates the computational and parameter burden introduced by DR layers but also avoids information loss, enhancing overall system efficiency and robustness.

Nes2Net incorporates a novel nested multi-scale design that enables more effective feature extraction and deeper cross-channel interactions without increasing model complexity. The improved Nes2Net-X further strengthens representation learning by introducing learnable weighted feature fusion, offering adaptive control over the feature aggregation process.

We conduct extensive evaluations across five representative datasets—CtrSVDD, ASVspoof 2021, ASVspoof 5, PartialSpoof, and In-the-Wild—covering a wide range of singing voice deepfakes, fully spoofed speech, adversarial attack, real-world deepfakes, and partially spoofed speech. Across all

scenarios, our models achieve SOTA performance, demonstrating superior generalization, compactness, and resilience under unseen and challenging conditions.

In summary, Nes2Net and Nes2Net-X offer a general-purpose, resource-efficient back-end for foundation model-based speech anti-spoofing, providing a practical yet powerful alternative to DR-dependent designs. To support future research and application, we make all source code and pre-trained models publicly available.

REFERENCES

- [1] A. Baevski, Y. Zhou, A. Mohamed, and M. Auli, “wav2vec 2.0: A framework for self-supervised learning of speech representations,” in *Proc. Adv. Neural Inf. Process. Syst. (NeurIPS)*, vol. 33, 2020, pp. 12 449–12 460.
- [2] W.-N. Hsu, B. Bolte, Y.-H. H. Tsai, K. Lakhotia, R. Salakhutdinov, and A. Mohamed, “HuBERT: Self-supervised speech representation learning by masked prediction of hidden units,” *IEEE/ACM Trans. Audio, Speech, Lang. Process.*, vol. 29, pp. 3451–3460, 2021.
- [3] S. Chen, C. Wang, Z. Chen, Y. Wu, S. Liu, Z. Chen, J. Li, N. Kanda, T. Yoshioka, X. Xiao, J. Wu, L. Zhou, S. Ren, Y. Qian, Y. Qian, J. Wu, M. Zeng, X. Yu, and F. Wei, “WavLM: Large-scale self-supervised pre-training for full stack speech processing,” *IEEE J. Sel. Top. Signal Process.*, vol. 16, no. 6, pp. 1505–1518, 2022.
- [4] A. T. Liu, S.-W. Li, and H.-y. Lee, “TERA: Self-supervised learning of transformer encoder representation for speech,” *IEEE/ACM Trans. Audio, Speech, Lang. Process.*, vol. 29, pp. 2351–2366, 2021.
- [5] J. Zhao and W.-Q. Zhang, “Improving automatic speech recognition performance for low-resource languages with self-supervised models,” *IEEE J. Sel. Top. Signal Process.*, vol. 16, no. 6, pp. 1227–1241, 2022.
- [6] J. weon Jung, W. Zhang, J. Shi, Z. Aldeneh, T. Higuchi, A. Gichamba, B.-J. Theobald, A. Hussen Abdelaziz, and S. Watanabe, “ESPnet-SPK: full pipeline speaker embedding toolkit with reproducible recipes, self-supervised front-ends, and off-the-shelf models,” in *Proc. INTERSPEECH*, 2024, pp. 4278–4282.
- [7] M. Li, Y. Ahmadi, and X.-P. Zhang, “A survey on speech deepfake detection,” *ACM Comput. Surv.*, vol. 57, no. 7, 2025.
- [8] N. M. Müller, P. Kawa, W. H. Choong, E. Casanova, E. Gölge, T. Müller, P. Syga, P. Sperl, and K. Böttinger, “MLAAD: The multi-language audio anti-spoofing dataset,” in *Proc. Int. Jt. Conf. Neural Netw. (IJCNN)*, 2024, pp. 1–7.
- [9] Y. Xie, Y. Lu, R. Fu, Z. Wen, Z. Wang, J. Tao, X. Qi, X. Wang, Y. Liu, H. Cheng, L. Ye, and Y. Sun, “The codefake dataset and countermeasures for the universally detection of deepfake audio,” *IEEE/ACM Trans. Audio, Speech, Lang. Process.*, vol. 33, pp. 386–400, 2025.
- [10] R. K. Das, X. Tian, T. Kinnunen, and H. Li, “The attacker’s perspective on automatic speaker verification: An overview,” in *Proc. INTERSPEECH*, 2020, pp. 4213–4217.
- [11] J.-w. Jung, Y. Wu, X. Wang, J.-H. Kim, S. Maiti, Y. Matsunaga, H.-j. Shim, J. Tian, N. Evans, J. S. Chung, W. Zhang, S. Um, S. Takamichi, and S. Watanabe, “SpoofCeleb: Speech deepfake detection and SASV in the wild,” *IEEE Open J. Signal Process.*, vol. 6, pp. 68–77, 2025.
- [12] J. Du, X. Chen, H. Wu, L. Zhang, I. Lin, I. Chiu, W. Ren, Y. Tseng, Y. Tsao, J.-S. R. Jang *et al.*, “CodecFake-Omni: A large-scale codec-based deepfake speech dataset,” *arXiv preprint arXiv:2501.08238*, 2025.
- [13] X. Chen, H. Wu, R. Jang, and H. yi Lee, “Singing voice graph modeling for singfake detection,” in *Proc. INTERSPEECH*, 2024, pp. 4843–4847.
- [14] Y. Zhu, S. Koppiseti, T. Tran, and G. Bharaj, “SLIM: Style-linguistics mismatch model for generalized audio deepfake detection,” in *Proc. Adv. Neural Inf. Process. Syst. (NeurIPS)*, vol. 37, 2024, pp. 67 901–67 928.
- [15] H. Tak, M. Todisco, X. Wang, J. weon Jung, J. Yamagishi, and N. Evans, “Automatic speaker verification spoofing and deepfake detection using wav2vec 2.0 and data augmentation,” in *Proc. Odyssey Speaker Lang. Recognit. Workshop*, 2022, pp. 112–119.
- [16] A. Guragain, T. Liu, Z. Pan, H. B. Sailor, and Q. Wang, “Speech foundation model ensembles for the controlled singing voice deepfake detection (CtrSVDD) challenge 2024,” in *Proc. IEEE Spoken Lang. Technol. Workshop (SLT)*, 2024.
- [17] Y. Xiao and R. K. Das, “XLSR-Mamba: A dual-column bidirectional state space model for spoofing attack detection,” *IEEE Signal Process. Lett.*, vol. 32, pp. 1276–1280, 2025.
- [18] S.-H. Gao, M.-M. Cheng, K. Zhao, X.-Y. Zhang, M.-H. Yang, and P. Torr, “Res2Net: A new multi-scale backbone architecture,” *IEEE Trans. Pattern Anal. Mach. Intell.*, vol. 43, no. 2, pp. 652–662, 2021.
- [19] K. He, X. Zhang, S. Ren, and J. Sun, “Deep residual learning for image recognition,” in *Proc. IEEE Conf. Comput. Vis. Pattern Recognit.*, 2016, pp. 770–778.
- [20] Y. Chen, S. Zheng, H. Wang, L. Cheng, Q. Chen, and J. Qi, “An enhanced Res2Net with local and global feature fusion for speaker verification,” in *Proc. INTERSPEECH*, 2023, pp. 2228–2232.
- [21] Y. Chen, S. Zheng, H. Wang, L. Cheng, Q. Chen, S. Zhang, and J. Li, “ERes2NetV2: Boosting short-duration speaker verification performance with computational efficiency,” in *Proc. INTERSPEECH*, 2024, pp. 3245–3249.
- [22] T. Liu, K. A. Lee, Q. Wang, and H. Li, “Golden Gemini is all you need: Finding the sweet spots for speaker verification,” *IEEE/ACM Trans. Audio, Speech, Lang. Process.*, vol. 32, pp. 2324–2337, 2024.
- [23] X. Li, X. Wu, H. Lu, X. Liu, and H. Meng, “Channel-wise gated Res2Net: Towards robust detection of synthetic speech attacks,” in *Proc. INTERSPEECH*, 2021, pp. 4314–4318.
- [24] J. Kim and S. M. Ban, “Phase-aware spoof speech detection based on Res2Net with phase network,” in *Proc. ICASSP*, 2023, pp. 1–5.
- [25] T. Liu, I. Kukanov, Z. Pan, Q. Wang, H. B. Sailor, and K. A. Lee, “Towards quantifying and reducing language mismatch effects in cross-lingual speech anti-spoofing,” in *Proc. IEEE Spoken Lang. Technol. Workshop (SLT)*, 2024, pp. 1185–1192.
- [26] J.-w. Jung, H.-S. Heo, H. Tak, H.-j. Shim, J. S. Chung, B.-J. Lee, H.-J. Yu, and N. Evans, “AASIST: Audio anti-spoofing using integrated spectro-temporal graph attention networks,” in *Proc. ICASSP*, 2022, pp. 6367–6371.
- [27] Y. Chen, J. Yi, J. Xue, C. Wang, X. Zhang, S. Dong, S. Zeng, J. Tao, Z. Lv, and C. Fan, “RawBMamba: End-to-end bidirectional state space model for audio deepfake detection,” in *Proc. INTERSPEECH*, 2024, pp. 2720–2724.
- [28] Y. Chen, H. Wu, N. Jiang, X. Xia, Q. Gu, Y. Hao, P. Cai, Y. Guan, J. Wang, W. Xie *et al.*, “Ustc-kxdigit system description for asvspoof5 challenge,” *arXiv preprint arXiv:2409.01695*, 2024.
- [29] Z. Wei, D. Ye, J. Deng, and Y. Lin, “From voices to beats: Enhancing music deepfake detection by identifying forgeries in background,” in *Proc. ICASSP*, 2025, pp. 1–5.
- [30] Y. Guan, Y. Ai, Z. Li, S. Peng, and W. Guo, “Recursive feature learning from pre-trained models for spoofing speech detection,” in *Proc. ICASSP*, 2025, pp. 1–5.
- [31] Z. Pan, T. Liu, H. B. Sailor, and Q. Wang, “Attentive merging of hidden embeddings from pre-trained speech model for anti-spoofing detection,” in *Proc. INTERSPEECH*, 2024, pp. 2090–2094.
- [32] M. Huzaifah, G. Lin, T. Liu, H. B. Sailor, K. M. Tan, T. K. Vangani, Q. Wang, J. H. M. Wong, N. F. Chen, and A. T. Aw, “MERaLiON-SpeechEncoder: Towards a speech foundation model for singapore and beyond,” 2024. [Online]. Available: <https://arxiv.org/abs/2412.11538>
- [33] D.-T. Truong, R. Tao, T. Nguyen, H.-T. Luong, K. A. Lee, and E. S. Chng, “Temporal-channel modeling in multi-head self-attention for synthetic speech detection,” in *Proc. INTERSPEECH*, 2024, pp. 537–541.
- [34] B. Desplanques, J. Thienpondt, and K. Demuyne, “ECAPA-TDNN: Emphasized channel attention, propagation and aggregation in TDNN based speaker verification,” in *Proc. INTERSPEECH*, 2020, pp. 3830–3834.
- [35] Q. Zhang, S. Wen, and T. Hu, “Audio deepfake detection with self-supervised XLS-R and SLS classifier,” in *Proc. ACM Int. Conf. Multimedia*, 2024, pp. 6765–6773.
- [36] Z. Ge, X. Xu, H. Guo, Z. Yang, and B. Schuller, “Gncl: A graph neural network with consistency loss for segment-level spoofed speech detection,” in *Proc. ICASSP*, 2025, pp. 1–5.
- [37] X. Wang, H. Delgado, H. Tak, J. weon Jung, H. jin Shim, M. Todisco, I. Kukanov, X. Liu, M. Sahidullah, T. H. Kinnunen, N. Evans, K. A. Lee, and J. Yamagishi, “ASVspoof 5: crowdsourced speech data, deepfakes, and adversarial attacks at scale,” in *Autom. Speaker Verif. Spoofing Countermeas. Workshop*, 2024, pp. 1–8.
- [38] Y. Zhang, Y. Zang, J. Shi, R. Yamamoto, T. Toda, and Z. Duan, “SVDD 2024: The inaugural singing voice deepfake detection challenge,” in *Proc. IEEE Spoken Lang. Technol. Workshop (SLT)*, 2024, pp. 782–787.
- [39] Q. Zhang, S. Wen, F. Yan, T. Hu, and J. Li, “XWSB: A blend system utilizing XLS-R and WavLM with SLS classifier detection system for SVDD 2024 challenge,” in *Proc. IEEE Spoken Lang. Technol. Workshop (SLT)*, 2024, pp. 788–794.
- [40] J. Yi, J. Tao, R. Fu, X. Yan, C. Wang, T. Wang, C. Y. Zhang, X. Zhang, Y. Zhao, Y. Ren *et al.*, “ADD 2023: the second audio deepfake detection challenge,” *arXiv preprint arXiv:2305.13774*, 2023.

- [41] J. Hu, L. Shen, and G. Sun, "Squeeze-and-excitation networks," in *Proc. IEEE Conf. Comput. Vis. Pattern Recog. (CVPR)*, 2018.
- [42] K. Okabe, T. Koshinaka, and K. Shinoda, "Attentive statistics pooling for deep speaker embedding," in *Proc. INTERSPEECH*, 2018, pp. 2252–2256.
- [43] T. Zhou, Y. Zhao, and J. Wu, "ResNeXt and Res2Net structures for speaker verification," in *Proc. IEEE Spoken Lang. Technol. Workshop (SLT)*, 2021, pp. 301–307.
- [44] Q. Wang, B. Wu, P. Zhu, P. Li, W. Zuo, and Q. Hu, "ECA-Net: Efficient channel attention for deep convolutional neural networks," in *Proc. IEEE Conf. Comput. Vis. Pattern Recog. (CVPR)*, 2020, pp. 11 531–11 539.
- [45] T. Liu, R. K. Das, K. A. Lee, and H. Li, "MFA: TDNN with multi-scale frequency-channel attention for text-independent speaker verification with short utterances," in *Proc. ICASSP*, 2022, pp. 7517–7521.
- [46] Y. Zang, J. Shi, Y. Zhang, R. Yamamoto, J. Han, Y. Tang, S. Xu, W. Zhao, J. Guo, T. Toda, and Z. Duan, "CtrSVDD: A benchmark dataset and baseline analysis for controlled singing voice deepfake detection," in *Proc. INTERSPEECH*, 2024, pp. 4783–4787.
- [47] X. Wang, J. Yamagishi, M. Todisco, H. Delgado, A. Nautsch, N. Evans, M. Sahidullah, V. Vestman, T. Kinnunen, K. A. Lee, L. Juvela, P. Alku, Y.-H. Peng, H.-T. Hwang, Y. Tsao, H.-M. Wang, S. L. Maguer, M. Becker, F. Henderson, R. Clark, Y. Zhang, Q. Wang, Y. Jia, K. Onuma, K. Mushika, T. Kaneda, Y. Jiang, L.-J. Liu, Y.-C. Wu, W.-C. Huang, T. Toda, K. Tanaka, H. Kameoka, I. Steiner, D. Matrouf, J.-F. Bonastre, A. Govender, S. Ronanki, J.-X. Zhang, and Z.-H. Ling, "ASVspooF 2019: A large-scale public database of synthesized, converted and replayed speech," *Comput. Speech Lang.*, vol. 64, p. 101114, 2020.
- [48] J. Yamagishi, X. Wang, M. Todisco, M. Sahidullah, J. Patino, A. Nautsch, X. Liu, K. A. Lee, T. Kinnunen, N. Evans, and H. Delgado, "ASVspooF 2021: accelerating progress in spoofed and deepfake speech detection," in *Autom. Speaker Verif. Spoofing Countermeas. Challenge*, 2021, pp. 47–54.
- [49] X. Wang, H. Delgado, H. Tak, J.-w. Jung, H.-j. Shim, M. Todisco, I. Kukanov, X. Liu, M. Sahidullah, T. Kinnunen *et al.*, "ASVspooF 5: Design, collection and validation of resources for spoofing, deepfake, and adversarial attack detection using crowdsourced speech," *arXiv preprint arXiv:2502.08857*, 2025.
- [50] N. M. Müller, P. Czempin, F. Dieckmann, A. Froghyar, and K. Böttinger, "Does audio deepfake detection generalize?" in *Proc. INTERSPEECH*, 2022, pp. 2783–2787.
- [51] L. Zhang, X. Wang, E. Cooper, N. Evans, and J. Yamagishi, "The PartialSpoof database and countermeasures for the detection of short fake speech segments embedded in an utterance," *IEEE/ACM Trans. Audio, Speech, Lang. Process.*, vol. 31, pp. 813–825, 2023.
- [52] Y. Zang, Y. Zhang, M. Heydari, and Z. Duan, "SingFake: Singing voice deepfake detection," in *Proc. ICASSP*, 2024, pp. 12 156–12 160.
- [53] Y. Xie, J. Zhou, X. Lu, Z. Jiang, Y. Yang, H. Cheng, and L. Ye, "FSD: An initial chinese dataset for fake song detection," in *Proc. ICASSP*, 2024, pp. 4605–4609.
- [54] H. Tak, M. Kamble, J. Patino, M. Todisco, and N. Evans, "Rawboost: A raw data boosting and augmentation method applied to automatic speaker verification anti-spoofing," in *Proc. ICASSP*, 2022, pp. 6382–6386.
- [55] D. P. Kingma and J. Ba, "Adam: A method for stochastic optimization," in *Int. Conf. Learn. Represent.*, 2015.
- [56] D. Snyder, G. Chen, and D. Povey, "Musan: A music, speech, and noise corpus," *arXiv preprint arXiv:1510.08484*, 2015.
- [57] T. Ko, V. Peddinti, D. Povey, M. L. Seltzer, and S. Khudanpur, "A study on data augmentation of reverberant speech for robust speech recognition," in *2017 IEEE international conference on acoustics, speech and signal processing (ICASSP)*. IEEE, 2017, pp. 5220–5224.
- [58] T. Liu, L. Zhang, R. K. Das, Y. Ma, R. Tao, and H. Li, "How do neural spoofing countermeasures detect partially spoofed audio?" in *Proc. INTERSPEECH*, 2024, pp. 1105–1109.
- [59] X. Wang and J. Yamagishi, "A comparative study on recent neural spoofing countermeasures for synthetic speech detection," in *Proc. INTERSPEECH*, 2021, pp. 4259–4263.
- [60] X. Glorot, A. Bordes, and Y. Bengio, "Deep sparse rectifier neural networks," in *Proc. Int. Conf. Artif. Intell. Stat.*, vol. 15, 2011, pp. 315–323.
- [61] D. Hendrycks and K. Gimpel, "Gaussian error linear units (gelus)," *arXiv preprint arXiv:1606.08415*, 2016.
- [62] S. Elfving, E. Uchibe, and K. Doya, "Sigmoid-weighted linear units for neural network function approximation in reinforcement learning," *Neural New.*, vol. 107, pp. 3–11, 2018.
- [63] G. Klambauer, T. Unterthiner, A. Mayr, and S. Hochreiter, "Self-normalizing neural networks," in *Proc. Adv. Neural Inf. Process. Syst. (NeurIPS)*, vol. 30, 2017.
- [64] J. M. Martín-Doñas and A. Álvarez, "The Vicomtech audio deepfake detection system based on wav2vec2 for the 2022 ADD challenge," in *Proc. ICASSP*, 2022, pp. 9241–9245.
- [65] X. Wang and J. Yamagishi, "Investigating self-supervised front ends for speech spoofing countermeasures," in *Proc. Odyssey Speaker Lang. Recognit. Workshop*, 2022, pp. 100–106.
- [66] E. Rosello, A. Gomez-Alanis, A. M. Gomez, and A. Peinado, "A conformer-based classifier for variable-length utterance processing in anti-spoofing," in *Proc. INTERSPEECH*, 2023, pp. 5281–5285.
- [67] E. Rosello, A. M. Gomez, I. López-Espejo, A. M. Peinado, and J. M. Martín-Doñas, "Anti-spoofing ensembling model: Dynamic weight allocation in ensemble models for improved voice biometrics security," in *Proc. INTERSPEECH*, 2024, pp. 497–501.
- [68] H. M. Tran, D. Guennec, P. Martin, A. Sini, D. Lolive, A. Delhay, and P.-F. Marteau, "Spoofed speech detection with a focus on speaker embedding," in *Proc. INTERSPEECH*, 2024, pp. 2080–2084.
- [69] B. Wang, Y. Tang, F. Wei, Z. Ba, and K. Ren, "FTDKD: Frequency-time domain knowledge distillation for low-quality compressed audio deepfake detection," *IEEE/ACM Trans. Audio, Speech, Lang. Process.*, vol. 32, pp. 4905–4918, 2024.
- [70] Y. Zhang, J. Lu, Z. Shang, W. Wang, and P. Zhang, "Improving short utterance anti-spoofing with AASIST2," in *Proc. ICASSP*, 2024, pp. 11 636–11 640.
- [71] Y. Guo, H. Huang, X. Chen, H. Zhao, and Y. Wang, "Audio deepfake detection with self-supervised WavLm and multi-fusion attentive classifier," in *Proc. ICASSP*, 2024, pp. 12 702–12 706.
- [72] Z. Wang, R. Fu, Z. Wen, J. Tao, X. Wang, Y. Xie, X. Qi, S. Shi, Y. Lu, Y. Liu *et al.*, "Mixture of experts fusion for fake audio detection using frozen wav2vec 2.0," *arXiv preprint arXiv:2409.11909*, 2024.
- [73] J. Lu, Y. Zhang, W. Wang, Z. Shang, and P. Zhang, "One-class knowledge distillation for spoofing speech detection," in *Proc. ICASSP*, 2024, pp. 11 251–11 255.
- [74] W. Huang, Y. Gu, Z. Wang, H. Zhu, and Y. Qian, "Generalizable audio deepfake detection via latent space refinement and augmentation," in *Proc. ICASSP*, 2025, pp. 1–5.
- [75] C. Y. Kwok, D.-T. Truong, and J. Q. Yip, "Robust audio deepfake detection using ensemble confidence calibration," in *Proc. ICASSP*, 2025, pp. 1–5.
- [76] Z. Jin, L. Lang, and B. Leng, "Wave-spectrogram cross-modal aggregation for audio deepfake detection," in *Proc. ICASSP*, 2025, pp. 1–5.
- [77] O. Pascu, A. Stan, D. Oneata, E. Oneata, and H. Cucu, "Towards generalisable and calibrated audio deepfake detection with self-supervised representations," in *Proc. INTERSPEECH*, 2024, pp. 4828–4832.
- [78] H.-T. Luong, H. Li, L. Zhang, K. A. Lee, and E. S. Chng, "LlamaPartial-Spoof: An LLM-driven fake speech dataset simulating disinformation generation," *arXiv preprint arXiv:2409.14743*, 2024.
- [79] T. Liu, K. A. Lee, Q. Wang, and H. Li, "Disentangling voice and content with self-supervision for speaker recognition," *Proc. Adv. Neural Inf. Process. Syst. (NeurIPS)*, vol. 36, pp. 50 221–50 236, 2023.
- [80] S. Wang, Z. Chen, K. A. Lee, Y. Qian, and H. Li, "Overview of speaker modeling and its applications: From the lens of deep speaker representation learning," *IEEE/ACM Trans. Audio, Speech, Lang. Process.*, vol. 32, pp. 4971–4998, 2024.